First-principles simulations of vibrational decay and lifetimes in *a*-Si:H and *a*-Si:D

Raymond Atta-Fynn,[1] David A. Drabold,[2] Stephen R. Elliott,[3] and Parthapratim Biswas[4]

[1]*Department of Physics, University of Texas, Arlington, TX 76019*[*]

[2]*Department of Physics and Astronomy, Ohio University, Athens, OH 45701*[†]

[3]*Department of Chemistry, University of Cambridge,*

Cambridge, CB2 1EW, United Kingdom[‡]

[4]*Department of Physics and Astronomy,*

The University of Southern Mississippi, Hattiesburg, MS 39406[§]

Abstract

Phonon lifetime in materials is an important observable that conveys basic information about structure, dynamics and anharmonicity. Recent vibrational transient-grating measurements, using picosecond infrared pulses from free-electron lasers, have demonstrated that the vibrational-population decay rates of localized high-frequency stretching modes (HSMs) in hydrogenated and deuterated amorphous silicon (*a*-Si:H/D) increase with temperature and the vibrational energy redistributes among the bending modes of Si in *a*-Si:H/D. Motivated by this observation, we address the problem from first-principles density-functional calculations and study the time evolution of the vibrational-population decay in *a*-Si:H/D, the average decay times and the possible decay channels for the redistribution of vibrational energy. The average lifetimes of the localized HSMs in *a*-Si:H and *a*-Si:D are found to be approximately 51–92 ps and 50–78 ps, respectively, in the temperature range of 25–200 K, which are consistent with experimental data. A weak temperature dependence of the vibrational-population decay rates has been observed via a slight increase of the decay rates with temperature, which can be attributed to stimulated emission and increased anharmonic coupling between the normal modes at high temperature.

PACS numbers: 71.23.Cq, 71.15.Mb, 71.23.An

I. INTRODUCTION

Classical normal modes have the essential property that they are a constant of the motion – in a harmonic system, such modes have an infinite lifetime. Of course, real materials experience anharmonic interactions which lead to energy transfer among the modes, and therefore a time dependence of the spectral weight of each mode, at least when the system is out of equilibrium. A picture of the energy-transfer mechanism is easily derived in perturbation theory, and leads to a considerable basic understanding, such as more rapid energy transfer for localized states near or in a continuum band of vibrational states. Such an analysis for small molecules shows the existence of new excitations with frequencies at sums and differences of the harmonic frequencies[1]. As the anharmonicity increases (presumably by driving the system harder or raising the temperature), additional frequencies appear, as seen in early *ab initio* studies of clusters[2]. If such a molecule were mechanically coupled to a solid with a phonon band containing any of the excitations, relatively rapid energy transfer would be expected, at least when it is not forbidden by symmetry.[3] Thus, while the basic picture of such energy transfer is clear enough, there is little precedent for calculations of predictive accuracy. In topologically disordered systems, such as hydrogenated amorphous silicon, the network dynamics are significantly more complex and environment-dependent than in crystals. Local vibrational amplitudes of the amorphous-silicon backbone vary significantly, and it may be expected that this leads to a larger sampling of the anharmonic part of the interatomic potential. This can be expected to have a non-trivial impact on mode lifetimes, which we are able to compute in a fairly quantitative way in this work.

Silicon has been at the forefront of the most important materials for photovoltaic production of electricity from solar energy. While crystalline silicon-based tandem solar cells have shown a promising way to overcome the Shockley-Queisser[4] limit of the conversion efficiency of single-junction solar cells, by using multiple p-i-n junctions for effective use of the solar spectrum, the complexity of designing multi-junction photovoltaic cells with several bandgaps has led to the development of alternative approaches, such as heterojunction intrinsic thin-layer (HIT) technology involving crystalline and amorphous silicon. Compared to crystalline silicon, amorphous silicon has a lower production cost and higher optical absorption coefficient, which make the latter a suitable candidate for thin-film solar cells. However, amorphous silicon is particularly sensitive to the light-induced structural degradation, which reduces efficiency and stability of *a*-Si:H-based solar cells upon prolonged illumination.[5] It has been suggested[6–8] that the dynamics of H atoms play a

crucial role in the photo-degradation of *a*-Si:H. Sugiyama et al.[6] have observed that the stability of *a*-Si:H-based solar cells improves considerably when hydrogen (H) atoms in the intrinsic layer of the cells are replaced by deuterium (D) atoms. Subsequent studies[7,8] have indicated that the strong coupling between the localized SiD wagging mode (at 510 cm^{-1}) and an extended Si-Si lattice mode (at 495 cm^{-1}) is responsible for fast dissipation of the photo-excited vibrational energy, which prevents local accretion of vibrational energy and reduces the dissociation probability of weak Si-Si or SiD bonds in the neighboring region. In contrast, a weak coupling between the corresponding SiH (at 640 cm^{-1}) and Si-Si modes in *a*-Si:H is often attributed to the build-up of vibrational energy locally, which promotes the degradation process by increasing the likelihood of breaking weak bonds in the vicinity. Thus, the vibrational dynamics of SiH/SiD bonds provide considerable information and new understanding of photo-degradation in these materials.

Recent vibrational transient-grating measurements on *a*-Si:D/H films, using intense picosecond pulses from a free-electron laser (FEL),[9–13] have revealed that the decay of the vibrational population of SiH stretching modes at low temperature shows a non-exponential character,[9–12] whereas the SiD stretching mode exhibits a single-exponential decay.[13] For *a*-Si:H, these observations are consistent with the results from two-dimensional infrared (2DIR) spectroscopy.[14] These experiments also indicate that the lifetime of the vibrational population in *a*-Si:D is lower than that in *a*-Si:H, and the decay rates–for both *a*-Si:H and *a*-Si:D–are weakly dependent on temperature. Further, the results suggest that the vibrational-energy relaxation of the SiH stretching mode proceeds by decaying into three SiH bending modes and one transverse-acoustic phonon,[9–12] while the SiD stretching mode decays directly into the collective Si-Si lattice modes of *a*-Si without exciting any SiD bending modes.[13]

In contrast to amorphous silicon, the vibrational-energy decay and the lifetime of the SiH/SiD modes in crystalline silicon have been studied extensively by a number of researchers using infrared absorption spectroscopy and transient bleaching spectroscopy.[15–19] The results from these studies indicate that the lifetimes of the H- and D-related stretching modes in crystalline silicon environment strongly depend on the nature of the H/D defect configurations. The experimental values of the lifetime of the SiH/SiD modes have been found to vary from 1.9 ps for the H_2^* defect configuration (2062 cm^{-1}) to 295 ps for the divacancy $HV{\cdot}VH_{110}$ (2072.5 cm^{-1}) configuration.[16] Furthermore, unlike in *a*-Si, the lifetimes of the SiD stretching modes in *c*-Si have been found to be longer than the corresponding SiH modes.[16] Similarly, the vibrational lifetimes of the H- and D-related bending modes have been measured by Sun et al.[19] using transient bleaching spectroscopy.

By analyzing the experimental data for SiH/SiD bending modes of H_2^* defects in crystalline Si and Ge, these authors have concluded that the lifetime of the bending modes increases exponentially with the number of phonons involved in the decay process and that the values of the lifetime range from 1 ps for a single-phonon process to 265 ps for a process involving four phonons.

While infrared absorption spectroscopy and ultrafast spectroscopy provide a clear picture of the vibrational-relaxation dynamics of H and D atoms in *c*-Si and *a*-Si, the majority of theoretical/computational studies on the vibrational lifetimes of SiH/SiD modes are focused on *c*-Si.[20–23] The vibrational dynamics of the SiH/SiD stretching modes, for several defect configurations in *c*-Si, such as H_2^*, D_2^*, VH·HV and VD·DV, have been studied by West and Estreicher[20,23] using *ab initio* molecular-dynamics simulations. The authors have computed the vibrational energy and the lifetimes of the SiH/SiD normal modes by employing an instantaneous normal-mode approximation that converts the $3N$ Cartesian coordinates of the atoms to the corresponding normal-mode coordinates. However, no first-principles study of the vibrational dynamics of SiH/SiD modes in *amorphous* silicon has been reported in the literature to the best of our knowledge. An earlier study of vibrational dynamics H and D atoms in *a*-Si:D/H, which employed tight-binding molecular-dynamics simulations, indicated that the SiD bonds were more stable than the SiH bonds but the study failed to observe any vibrational-energy decay over a simulation time of five picoseconds.[24] Inspired by the results from recent transient-grating experiments[9–13] on *a*-Si:D/H and our desire to address the problem from an *ab-initio* viewpoint, for direct comparison with the experimental results, we have conducted first-principles density-functional simulations of the vibrational population decay of SiH/SiD stretching modes in the amorphous-silicon environment. Toward that end, we have presented here a simulation methodology that is capable of exciting SiH/SiD stretching modes in a manner that approximately mimics ultrafast transient-grating experiments without using the harmonic approximation.

The rest of the paper is organized as follows. In section II, we have provided a detailed description of the computational methodology used for the calculation of vibrational lifetimes of SiH/SiD stretching modes using density-functional simulations. Section III discusses the results from our work with an emphasis on the nature of the vibrational-energy decay and the relaxation pathways or decay channels for high-energy SiH/SiD stretching modes. This is followed by the conclusions of our work in section IV.

II. COMPUTATIONAL METHODOLOGY

Car-Parrinello molecular dynamics (CPMD)[25] simulations were carried out in the canonical ensemble (at selected temperatures) and microcanonical ensemble for two independent structural models: an *a*-Si:H model with 10.7 at. % H and an *a*-Si:D model with 12.2 at. % D. The models were generated using a recently developed metadynamical approach,[26] which is capable of producing high-quality networks of *a*-Si:H/D,[26] coupled with *ab initio* interactions. The CPMD simulations are based on the density-functional theory (DFT) of Kohn and Sham,[27,28] which employs norm-conserving pseudopotentials and plane-wave basis functions, as implemented within the NWCHEM code.[29] The exchange-correlation contribution to the total energy was taken into account by using a generalized-gradient approximation (GGA) as formulated by Perdew, Burke and Ernzerhof (PBE).[30] Electron-ion interactions were treated using norm-conserving pseudopotentials, which were modified into a separable form due to Kleinman and Bylander.[31] The Kohn-Sham wave functions and charge density were expanded using plane-wave basis functions with a kinetic-energy cutoff of 50 and 100 Ry, respectively. The Γ point of the k-space was used to sample the Brillouin zone in all simulations.[32] In the description of all CPMD simulations to follow, we chose an integration time step of δt = 5 a.u. (0.121 fs) and a fictitious electronic mass of 600 a.u. for the time evolution of the electronic degrees of freedom. The simulation temperature was controlled using a chain of Nosé-Hoover thermostats,[33–35] which accurately produces atomic dynamics in canonical ensembles. Since direct simulations of an actual experiment in ultrafast spectroscopy, namely the excitation of high-frequency SiH modes in *a*-Si:H at or near 2000 cm^{-1} by using a tunable, ultrafast, free-electron laser (FEL) with a spectral width of a few tens of cm^{-1} is highly nontrivial, we proceed with the assumption that the excitation of the stretching modes is possible by depositing energy locally into the SiH bonds that vibrate in the frequency range of 1950-2150 cm^{-1} from a Gaussian distribution with a mean equal to the average energy of the stretching modes (2000 cm^{-1}) and a width reflecting the frequency range of the modes. Thus, our simulation consists of the following steps:

1) **Structural relaxations and vibrational normal-mode calculations**: The configurations of *a*-Si:H/D were relaxed until the atomic force on each atom was less than 0.005 eV/Å. For each relaxed configuration, the dynamical-matrix elements were computed in the harmonic approximation by successively displacing each atom in the supercell along three orthogonal directions by 0.01 a.u. (0.0529 Å). The resulting dynamical matrix was diagonalized to obtain the vibrational

eigenfrequencies and eigenvectors. The eigenvalues of the dynamical matrices of *a*-Si:H and *a*-Si:D were found to be all positive indicating that none of the configurations had any imaginary frequency;

2) **Equilibrations using CPMD in the canonical ensemble**: For thermal equilibrium, each configuration was subjected to a constant-temperature CPMD run at five or six different temperatures within the range of 25-200 K. The equilibration at a given temperature lasted for about 12–15 ps. The purpose of this step is to ensure that thermal equilibrium is achieved both *locally* and *globally* so that the system does not have any 'hot' carriers or considerable local thermal fluctuations that might affect the vibrational-population decay;

3) **Post-equilibration unperturbed microcanonical CPMD**: After the equilibration in step 2, the final output (atomic coordinates and velocities) of each system was subjected to constant-energy dynamics[36] to eliminate any thermostat effects. The atomic trajectory was saved for every 10 time steps, which was subsequently used to compute the kinetic-energy decay upon infrared excitation, as described in step 5. The length of the trajectory was chosen to be at least 50 ps. During this time, the average temperature of each run was monitored, both locally and globally, and was found to be very close to the temperature of the parent configuration in step 2;

4) **Post-equilibration perturbed microcanonical CPMD**: In order to excite the SiH (SiD) vibrational stretching modes, following step 2, the velocities of Si and H (D) atoms of SiH (SiD) bonds were multiplied by an appropriate scale factor to deposit (infrared) energy in the system. To achieve this, the velocity scaling is performed in such a way that the additional (kinetic) energy deposited locally into an SiH (SiD) bond is equal to the energy of the vibrational (stretching) mode to be excited. Since there exists a band of stretching modes, one may choose the energy from a Gaussian distribution with a mean value $\hbar\omega_0$, where ω_0 is the characteristic vibrational frequency of the SiH (SiD) stretching modes. The width of the Gaussian distribution, σ, can be determined by the frequency range $\Delta\omega$ of the stretching modes. Here, we have used $\Delta\omega$ = 200 cm^{-1}, and $\sigma = \Delta\omega/5$ = 40 cm^{-1} (see Ref. 37). Thus, the Gaussian parameters for the SiH (SiD) system are given by ω_0=2000 (1460) cm^{-1} and σ = 40 cm^{-1}. The value of σ can be tuned depending upon the width of the stretching modes and it is reflective of the spectral width of FEL pulses used in actual pump-probe measurements in time-resolved spectroscopy. Once the velocity scaling of each SiH (SiD) bond was completed, the system was subjected to a constant-energy CPMD run. As in step 3, the trajectory for this perturbed dynamics was saved after every 10 time steps for the next 50 ps. Thus, our simulations generated atomic trajectories with a temporal resolution of 1.21 fs, which is

TABLE I. Structural properties of a-Si:D/H models used in this work. N is the number of atoms, C is the hydrogen/deuterium concentration (at. %), $R_{\mathrm{Si-X}}$ (X=H, D) is the average Si-X bond length. θ, $\Delta\theta$ and C_4 are the average bond angle, standard deviation of θ and the atomic concentration of four-fold coordinated Si atoms, respectively.

	N	C	$R_{\mathrm{Si-Si}}$	$R_{\mathrm{Si-X}}$	θ	$\Delta\theta$	C_4
a-Si:H	112	10.7	2.369	1.497	109.2	10.16	100
a-Si:D	114	12.2	2.374	1.496	109.1	10.33	100

sufficient for determining the characteristic features of vibrational energy decays;

5) **Computation of vibrational population lifetime**: The lifetime of the vibrational excitation of the SiH/SiD stretching vibrations can be obtained from the decay of the kinetic energy (KE) in the perturbed microcanonical runs in step 4. To minimize the effect of the KE fluctuations on the decay rate, the trivial contribution of the KE from the unperturbed run (in step 3) is subtracted to form,[38]

$$\delta_E(t,T) = \sum_{i\in\{\text{Si-H/Si-D}\}} \left[E^i_{\mathrm{p}}(t,T) - E^i_{\mathrm{u}}(t,T)\right], \tag{1}$$

where $E^i_{\mathrm{u}}(t,T)$ and $E^i_{\mathrm{p}}(t,T)$ are the kinetic energy of an SiH/SiD bond i in the unperturbed and perturbed constant-energy runs at temperature T in step 3 and 4, respectively. We have verified that the inclusion of the neighboring bonds in Eq. (1) does not affect the final results to an appreciable extent. Following van der Voort *et al.*[10] and Jobson *et al.*[12], the average lifetime, $\tau(T)$, of the excited SiH/SiD stretching vibrations at temperature T can be written as,

$$\tau(T) = \frac{2\int_0^\infty t\,\delta_E(t,T)}{\int_0^\infty \delta_E(t,T)}, \tag{2}$$

and the vibrational-population decay rate at temperature T is given by the reciprocal of $\tau(T)$. A multiplication factor 2 is included in the numerator in order to be consistent with the definition of τ in Refs. 9, 10, and 13 for the purpose of comparison with experimental data therein. In actual numerical calculations, the upper limit of the integrals in Eq. (2) is replaced by the total simulation time in step 3 or 4.

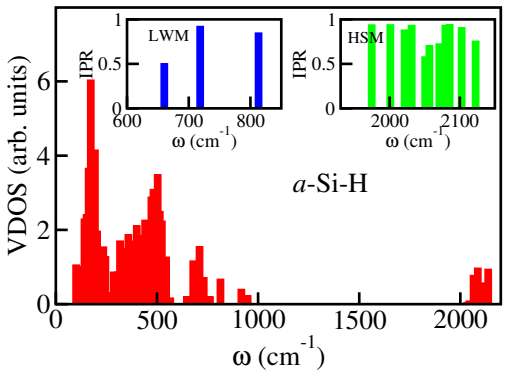

FIG. 1. Vibrational density of states for the *a*-Si:H model obtained using the harmonic approximation. The high-frequency stretching modes (HSM) appear in the vicinity of 2000 cm^{-1}, as indicated in the inset (right). Three low-frequency wagging modes (LWM) are also shown in the left inset. The degree of localization of the stretching/wagging modes (in the insets) is reflected in the corresponding IPR values.

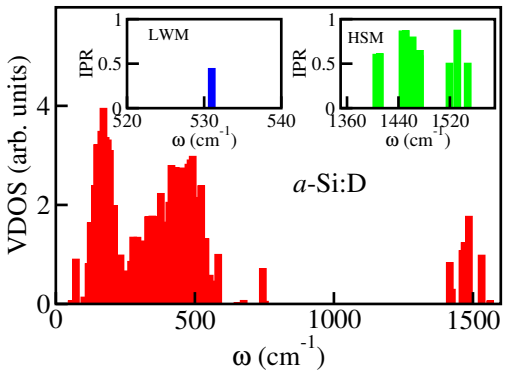

FIG. 2. Vibrational density of states for the *a*-Si:D model obtained using the harmonic approximation. The frequency positions of a few high-frequency stretching modes (HSM) and a low-frequency wagging mode (LWM) are shown in the right and left insets, respectively. The IPR values in the insets are indicative of the degree of localization of the modes.

III. RESULTS AND DISCUSSION

Table I lists the key structural properties of the *a*-Si:D/H models used in our simulations. Since CPMD simulations are computationally very expensive, and the simulation of vibrational dynamics requires a very small time step—a fraction of a femtosecond—with a total simulation time of several tens of picoseconds for our present purpose, we have restricted ourselves to models with 100 Si atoms containing 12 H and 14 D atoms. The vibrational densities of states (VDOS) for these models, obtained using the harmonic approximation, are shown in Figs. 1 and 2. A small band of

isolated states in the vicinity of 2001 (1450) cm^{-1} indicates the presence of high-frequency stretching modes (HSM) due to the vibration of SiH (SiD) bonds. To ensure that our models correctly produce the localized and stretching character of SiH (SiD) vibrations, we have examined the vibrational eigenfunctions and calculated the inverse participation ratio (IPR)[39] of the modes near 2001 (1460) cm^{-1}. The results confirmed that the modes are truly localized and the SiH (SiD) vibrations have a stretching character. An example of such a high-frequency stretching mode (2001 cm^{-1}) of SiH is shown in Fig.3 (cf. Fig. 1 in the inset for ω = 2001 cm^{-1}). The HSM is found to be highly localized with 97% of the total squared amplitude of the mode centered on the H atom and an analysis of the eigenvector reveals that the mode has 99.2% stretching character. Once the localized HSMs were identified, the (infrared) excitation of the HSMs proceeded using the method described in step 4 of section II. In view of the small number of modes near 2001 cm^{-1} (for SiH) and 1460 cm^{-1} (for SiD), we have not distinguished low-frequency stretching modes (LSM) from high-frequency stretching modes (HSM), and used the term HSM to indicate both of these modes hereafter. It may be noted that, although the VDOS in Figs. 1 and 2 have been obtained using the harmonic approximation, the vibrational lifetimes computed in this work are independent of the harmonic approximation. Since we do not compute the vibrational energy using the normal-mode frequencies and eigenvectors, the results include any possible anharmonic effects that might be present in the systems. The VDOS simply confirms the frequency position, vibrational character and the localized nature of the SiH/SiD stretching modes, which are implicitly assumed in writing Eq.(1).

A. Vibrational relaxation of SiH/SiD stretching modes

Figure 4 depicts the variation of $\delta_E(t, T)$ with time (t) in a-Si:H for three different temperatures T. The corresponding semi-log plots are also shown in the inset to characterize the energy decay. All the plots show a transient decay for the first few picoseconds, which are not included in the semi-log plots. A close examination of the plots in Fig. 4 reveals the following features: 1) the energy decay is temperature dependent – the higher the temperature, the faster the decay; 2) the decay appears to be multi-exponential in nature. This is particularly evident from the semi-log plots for temperatures 25 K and 200 K, where the presence of two characteristic time scales can be seen clearly (from 5 ps to 10–12 ps and 12 ps to 50 ps); 3) the remaining plot at T = 100 K appears to fit neither a single exponential nor a bi-exponential function. Although our results have

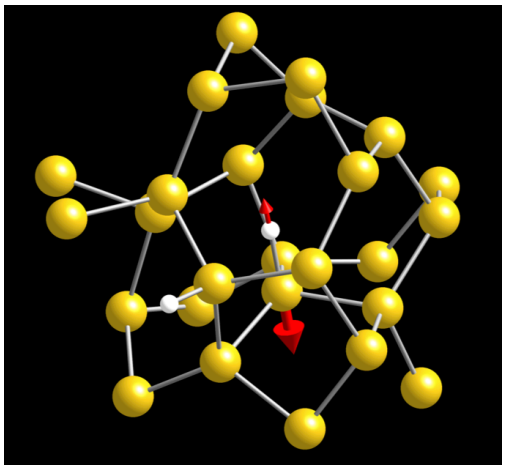

FIG. 3. A high-frequency localized SiH stretching mode, with 99.2% stretching character, observed at 2001 cm^{-1} in the a-Si:H model. Silicon and hydrogen atoms are shown in yellow and white colors, respectively.

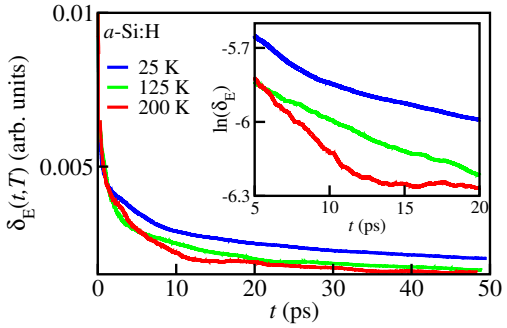

FIG. 4. The decay of vibrational energy $\delta_E(t,T)$ with time (t) in a-Si:H for three different temperatures T. The inset shows the corresponding plots on a semi-log scale.

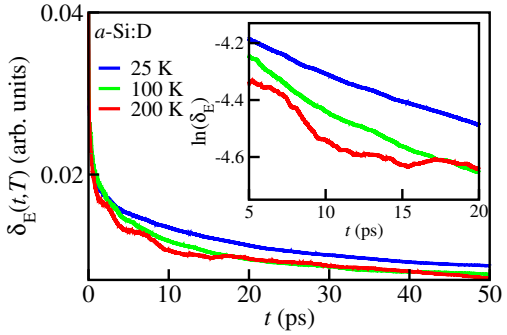

FIG. 5. Vibrational energy flow $\delta_E(t,T)$ as a function of time (t) for a-Si:D for temperatures T as indicated. The corresponding semi-log plots are shown in the inset.

been affected by the finite-size effects and limited statistics due to the presence of only a few H atoms in the model, it is apparent that the decay curves, in general, cannot be represented reliably by a single exponential function. This observation is in agreement with experimental studies on infrared transient-grating measurements of vibrational dynamics in *a*-Si:H thin films.[10–12] The corresponding variation of $\delta_E(t,T)$ for *a*-Si:D is shown in Fig. 5. While $\delta_E(t,T)$ for different temperatures shows a similar behavior as observed in the case of *a*-Si:H, there are subtle differences, which are particularly pronounced at low temperature, specifically at 25 K. A comparison of the semi-log plot for T = 25 K in Fig.5 with that from *a*-Si:H at the same temperature (in Fig. 4) suggests that the energy decay for *a*-Si:D exhibits a stronger linear behavior on the semi-log scale than for *a*-Si:H. In other words, the low-temperature (25 K) behavior of the vibrational-energy decay in *a*-Si:D can be adequately expressed by a single-exponential function. The deviation from a single-exponential behavior at high temperature can be largely attributed to the presence of strong anharmonic coupling and stimulated emissions. We should mention at this point that the single-exponential behavior of the vibrational-energy decay has been observed experimentally only at low temperature[13] to our knowledge. To examine this aspect further, we have directly compared our results from CPMD simulations at 25 K with the experimental data from infrared transient-grating measurements on *a*-Si:D at 4 K, obtained by Wells et al.,[9,13] in Fig. 6. The plots show that the simulated energy decay at 25 K is considerably slower than the experimental decay measured at 4 K. One plausible explanation for this slow behavior in simulation could be the absence of very low-energy Si modes in small models containing only $\sim$ 100 Si atoms and intrinsic quantum effects associated with the atomic dynamics of hydrogen/deuterium at low temperatures. Should the principal decay channels involve any low-energy modes that are missing, the absence of such modes would impede the dissipation process, particularly at low temperatures (due to weak anharmonic coupling between the modes), and affect the overall decay behavior by increasing the decay time. While our results do not match accurately with the experimental data at a quantitative level, there is a considerable agreement at the qualitative level. This is evident from Table II, where we have listed the computed values of the lifetimes of SiH and SiD stretching vibrations, along with the corresponding experimental values from Refs. 12 and 13, respectively. It may be noted that some of the experimental values provided in Table II were not obtained exactly at the simulated temperatures listed therein.

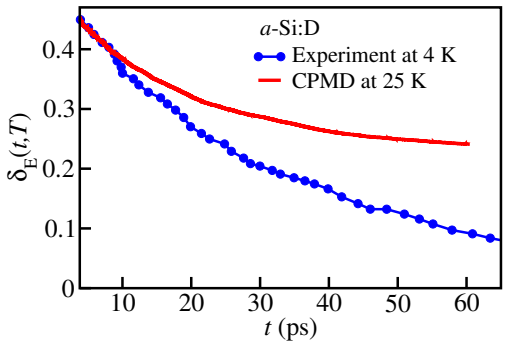

FIG. 6. Comparison of the decay of vibrational energy in *a*-Si:D from CPMD simulations at 25 K with the infrared transient-grating signal for resonant excitations of the *a*-Si:D stretching mode at 1461 cm^{-1}.

TABLE II. Average lifetimes of SiH (2000 cm^{-1}) and SiD (1460 cm^{-1}) stretching vibrations at selected temperatures. τ_{CPMD} and τ_{EXPT} denote the CPMD and experimental lifetimes, respectively. Experimental values are from Refs. 12 and 13. Experimental temperatures for some τ values are indicated where applicable.

			a-Si:H		
T (K)	25	75	100	125	200
τ_{CPMD} (ps)	78.1	92.0	73.1	74.0	51.3
τ_{EXPT} (ps)	101.1	93.7	82.7	72.7	57.3
			a-Si:D		
T (K)	25	75	100	125	200
τ_{CPMD} (ps)	78.7	54.0	54.6	–	50.1
τ_{EXPT} (ps)	56.2[a]	54.9[b]	57.1	–	52.8[c]

[a] Measured at T=40 K

[b] Measured at T=69.5 K

[c] Measured at T=189 K

B. Temperature dependence of lifetimes and decay channels

The temperature dependence of the decay rate, $1/\tau$, can be obtained by calculating τ using Eqs. (1) and (2). The results from our calculations are presented in Figs. 7 and 8 for *a*-Si:H and *a*-Si:D, respectively. Also included in these figures are the experimental data from infrared transient-

grating measurements by Jobson et al. [12] and Wells et al. [13] For *a*-Si:H, the agreement between computed values and experiment data is reasonably good with the exception of the decay rate at 25 K, where a considerable deviation from the experimental value has been observed. A similar deviation can be noticed for the case of *a*-Si:D at 25 K in Fig. 8 as well. While the origin of this deviation at low temperature is unknown to us, we surmise that the deviation can be attributed to the quantum-mechanical nature of the dynamics of light H/D nuclei that cannot fully treated classically at low temperature.[40] A path-integral Monte Carlo study of *a*-Si by Herrero,[41] which treats atomic nuclei as quantum particles, has indicated that the vibrational energy and the spatial delocalization of silicon atoms are indeed affected by non-trivial quantum effects and the anharmonic nature of atomic vibrations in the amorphous state. In view of this, it is not surprising that the results show noticeable fluctuations from the experimental data. Furthermore, the absence of very low-energy vibrational modes in the system could also be a possible contributing factor for this deviation to appear at low temperature. However, it is notable that the overall temperature dependence of the simulated decay rates, for both *a*-Si:H and *a*-Si:D, displays a qualitative behavior which is consistent with experimental observations.[12,13]

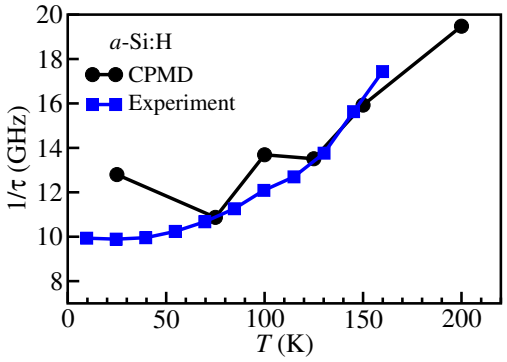

FIG. 7. Temperature dependence of the vibrational-energy decay rate for *a*-Si:H from CPMD simulations. Experimental data, due to Jobson et al. ,[12] are included for comparison.

When an atom or molecule is excited to its characteristic vibrational frequency ω in a condensed-phase system, the system relaxes via redistribution and delocalization of the vibrational energy through a number of possible decay channels comprising a few accepting modes ω_i of the surrounding phonon bath, such that the total energy is conserved in the process. While the exact relaxation process and the number of phonons involved in amorphous systems can be highly complicated, it is generally determined by the availability of accepting low-energy modes in the vibrational density of states and the anharmonic coupling between the decaying and accepting

modes. Following Nitzan et al. ,[42] a simple model of vibrational relaxation dynamics in condensed phases gives the following temperature dependence of the decay rate:

$$\frac{1}{\tau(T)} = \frac{1}{\tau(0)} \frac{\exp(\hbar\omega/k_B T) - 1}{\prod_{i=1}^{n} [\exp(\hbar\omega_i/k_B T) - 1]}. \tag{3}$$

Here $1/\tau(0)$ is the spontaneous decay rate in the limit $T \rightarrow 0$, which is generally approximated by the value of τ obtained at the lowest measured or computed temperature. Recently, several workers[9–13] have attempted to identify possible decay channels of SiH/SiD stretching modes in *a*-Si:D/H, involving three- or four-phonon processes, by fitting experimental data of the temperature dependence of vibrational relaxation rates of *a*-Si:D/H with Eq. (3). Here, we have adopted a similar approach to examine a few possible relaxation pathways, including those proposed by others, that satisfy the following conditions: 1) the relaxation process is energy conserving, $\sum_{i=1}^{n} \hbar\omega_i = \hbar\omega$; 2) the accepting mode ω_is are in ample supply, i.e., they correspond to the high-density regions of the vibrational density of states. While these "sum rules" cannot determine the decay channel(s) uniquely, they certainly reduce the number of possible combinations considerably. By invoking additional assumptions (e.g., the localized or delocalized nature of the accepting modes) and using Eq. (3), it is possible to study the presence of a few probable decay channels in the system. In our work, $\tau(0)$ was taken to be the decay rate at 25 K, which is found to be 12.8 GHz (12.7 GHz) for *a*-Si:H (*a*-Si:D).

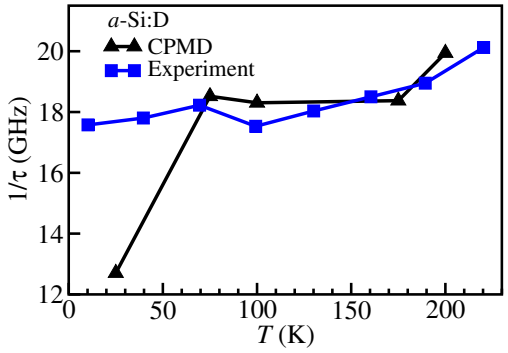

FIG. 8. Vibrational-energy decay rates as a function of temperature for *a*-Si:D. The experimental data are due to Wells et al. [13]

The results from our analysis, using Eq. (3), for the case of *a*-Si:H are presented in Fig. 9, where we have explored three decay channels. The first channel, indicated as A (in Fig. 9), comprises three SiH bending modes at 623 cm^{-1} and one Si-Si transverse-acoustic (TA) mode at 133 cm^{-1}. This channel was proposed by van der Voort et al. [10] in an effort to fit their experimental data from

infrared transient-grating and photon-echo measurements with Eq. (3). While the channel seems to produce the correct qualitative behavior of $\tau(T)$ with temperature, our CPMD data cannot be described very accurately by this channel. The second channel (C), proposed by Rella et al. ,[11] consists of four transverse-optical (TO) modes of 500 cm^{-1}. However, this produces a considerably weaker temperature dependence and it cannot explain the general behavior of $\tau(T)$, particularly at elevated temperatures. We thus propose a new decay channel (B) that involves one SiH bending mode at 623 cm^{-1}, one TO mode at 500 cm^{-1}, and three Si-Si longitudinal-acoustic (LA) modes at 301 cm^{-1}. The proposed channel satisfies the decay conditions mentioned earlier and provides a way of redistributing energy to the low-energy accepting modes in *a*-Si:H. Although it is unlikely to have high-order phonon processes at low temperature, the ample supply of Si-Si LA modes (at 301 cm^{-1}) in the vibrational density of states of *a*-Si:H makes this channel a likely candidate for a possible relaxation path for the vibrational energy relaxation of SiH stretching modes. Thus, despite the presence of some fluctuations and other shortcomings of our CPMD simulations, it is reasonable to conclude that both channel A and channel B provide a good choice for the possible decay channels for vibrational relaxation of high-frequency stretching modes near 2000 cm^{-1} in *a*-Si:H.

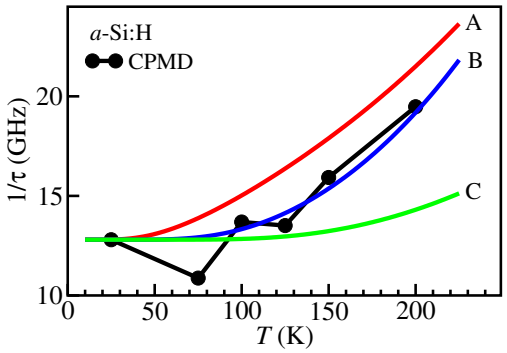

FIG. 9. The average decay rate from Eq. (3) for three decay channels discussed in the text: A) Three SiH bending modes at 623 cm^{-1} and one Si-Si TA phonon at 133 cm^{-1}; B) One SiH bending mode at 623 cm^{-1}, one TO phonon of 500 cm^{-1} and three Si-Si LA phonons at 301 cm^{-1}; C) four TO phonons of 500 cm^{-1}. Computed data are shown as black circles.

The decay channels for *a*-Si:D are depicted in Fig. 10. Earlier works by Wells et al. [9,13] have indicated that the relaxation of the vibrational energy from high-frequency stretching modes in *a*-Si:D takes place by circumventing the SiD bending modes, which causes the energy to drain into delocalized Si-Si modes and, consequently, leads to a relatively fast decay of vibrational en-

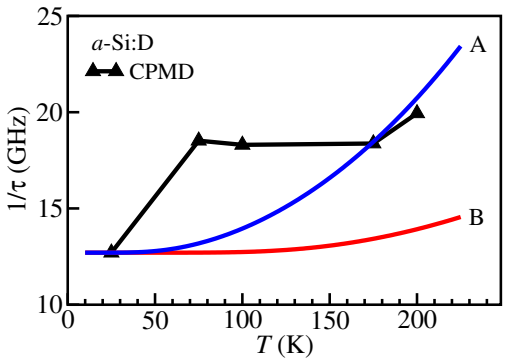

FIG. 10. Temperature dependence of the average decay rate for two decay channels in a-Si:D: A) four Si-Si modes (one at 335 cm^{-1}, one TA mode at 175 cm^{-1} and two TO modes at 485 cm^{-1}); B) three Si-Si modes each at 487 cm^{-1}. Simulated values are shown as black triangles.

ergy. However, unlike for a-Si:H, we could not find an appropriate channel for a-Si:D that fits our simulated data and satisfies the decay rules mentioned earlier owing to the presence of too much noise in the computed average lifetimes. Instead, here we choose to study two decay channels proposed by Wells et al. [9,13] and examine the correctness of our results. The temperature dependence of $\tau(T)$ for the channels are shown in Fig. 10. The first channel (A) involves four Si-Si modes comprising one at LA mode at 335 cm^{-1}, one TA mode at 175 cm^{-1} and two TO modes at 485 cm^{-1}, whereas the second channel (B) consists of three Si-Si modes each at 487 cm^{-1}. Although our results do not match well with the experimental data from Ref. 9, the computed values from CPMD simulations are reasonably close to the values obtained from channel A. Further simulation studies are needed to improve the statistics of our results for several temperatures in order to predict a possible decay channel in a-Si:D. Finally, it would be relevant to mention at this point that the lifetimes of the H- and D-related stretching modes in crystalline silicon also decrease with the increase of the temperature of the system. However, a direct comparison of the lifetimes of the SiH/SiD stretching modes in a-Si with those in c-Si is rather non-trivial owing to considerable differences between the local and global atomic structures, as well as the localization character of the vibrational modes in these systems.

IV. CONCLUSIONS

The vibrational relaxation of high-frequency stretching modes in a-Si:H and a-Si:D has been studied using first-principles density-functional calculations with particular emphasis on the decay

of the vibrational energy of stretching modes and the temperature dependence of the lifetime of the vibrational-population decay. Using Car-Parrinello molecular-dynamics (CPMD) simulations, combined with realistic models of *a*-Si:H and *a*-Si:D, we have observed that the decay behavior of the vibrational energy from high-frequency stretching modes is distinctly different in *a*-Si:H and *a*-Si:D. For *a*-Si:H, the time evolution of the vibrational energy appears to be largely bi- or multi-exponential in nature, whereas an almost single-exponential decay has been observed in *a*-Si:D at low temperature. The average lifetimes of the SiH and SiD stretching vibrations have been found to be approximately 51-78 ps and 57–70 ps, respectively, which approximately agree with experimental data in the temperature range of 25–200 K. In agreement with the experimental data from infrared transient-grating measurements, the simulated decay rates in *a*-Si:H and *a*-Si:D show a minor increase at elevated temperatures, which can be attributed to an increase of anharmonic coupling and the presence of stimulated emissions at high temperature. Using a simple theoretical model of vibrational relaxation in condensed-phase systems proposed elsewhere, an analysis of our results for *a*-Si:H suggests that the redistribution of vibrational energy takes place through two principal decay channels or relaxation pathways. The first channel involves three SiH bending vibrations at 623 cm^{-1} and one Si-Si vibration at 133 cm^{-1}, whereas the second channel comprises three Si-Si vibrations at 301 cm^{-1}, one SiH mode at 623 cm^{-1} and one Si-Si vibration at 500 cm^{-1}. While the presence of sizeable fluctuations in the temperature-dependence plot of the average decay rate in *a*-Si:D prevents us from proposing a definitive decay channel in this system, a combination of simulated and experimental data appear to suggest that four Si-Si modes (comprising one at 335 cm^{-1}, one TA mode at 175 cm^{-1} and two TO modes at 485 cm^{-1}) and three Si-Si vibrations at 487 cm^{-1} constitute the primary decay channels in *a*-Si:D. In conclusion, we have presented a fairly accurate first-principles simulation of vibrational-energy decay and lifetimes of high-frequency SiH/SiD vibrations in hydrogenated/deuterated amorphous silicon. By employing a simple mode-excitation scheme, which does not invoke the harmonic approximation and closely mimics time-resolved ultrafast infrared experiments using picosecond laser pulses, a quantitative agreement with experimental data has been obtained. The results presented here provide fundamental insight and understanding of the vibrational dynamics of hydrogen and deuterium atoms in amorphous silicon, which are particularly useful in technological development and designing of *a*-Si:H-based photovoltaic devices.

V. ACKNOWLEDGEMENTS

The work is partially supported by the U.S. National Science Foundation under Grants No. DMR 1507166, No. DMR 1507118, and No. DMR 1507670. We acknowledge the use of computing resources at the Texas Advanced Computing Center and Ohio Supercomputer Center.

---

* attafynn@uta.edu

† drabold@ohio.edu

‡ sre1@cam.ac.uk

§ partha.biswas@usm.edu; Corresponding author

[1] L. D. Landau and E. M. Lifshitz, *Mechanics, Course of Theoretical Physics, Vol 1, Third Edition* (Pergamon, Oxford, 1976).

[2] D. A. Drabold, S. Klemm, and O. F. Sankey, MRS Proceedings **193**, 177 (1990).

[3] The essential physical picture for spectral diffusion in NMR "hole burning" experiments and spectral diffusion among Kohn-Sham states is very similar to the problem encountered here.

[4] W. Shockley and H. J. Queisser, J. Appl. Phys. **32**, 510 (1961).

[5] D. L. Staebler and C. R. Wronski, Appl. Phys. Lett. **31**, 292 (1977).

[6] S. Sugiyama, J. Yang, and S. Guha, Appl. Phys. Lett. **70**, 378 (1997).

[7] J.-H. Wei, M.-S. Sun, and S.-C. Lee, Appl. Phys. Lett. **71**, 1498 (1997).

[8] A. Shih, S.-C. Lee, and C. Chia, Appl. Phys. Lett. **74**, 3347 (1999).

[9] J.-P. R. Wells, E. D. van Hattum, R. E. I. Schropp, P. J. Phillips, D. A. Carder, F. H. P. M. Habraken, and J. I. Dijkhuis, Phys. Stat. Sol. (b) **241**, 3474 (2004).

[10] M. van der Voort, C. W. Rella, L. F. G. van der Meer, A. V. Akimov, and J. I. Dijkhuis, Phys. Rev. Lett. **84**, 1236 (2000).

[11] C. W. Rella, M. van der Voort, A. V. Akimov, A. F. G. van der Meer, and J. I. Dijkhuis, Appl. Phys. Lett. **75**, 2945 (1999).

[12] K. W. Jobson, J.-P. R. Wells, R. E. I. Schropp, N. Q. Vinh, and J. I. Dijkhuis, J. Appl. Phys. **103**, 013106 (2008).

[13] J.-P. R. Wells, R. E. I. Schropp, L. F. G. van der Meer, and J. I. Dijkhuis, Phys. Rev. Lett. **89**, 125504 (2002).

[14] R. J. Scharff and S. D. McGrane, Physical Review B **76**, 054301 (2007).

[15] M. Budde, G. Lüpke, C. Parks Cheney, N. H. Tolk, and L. C. Feldman, Phys. Rev. Lett. **85**, 1452 (2000).

[16] M. Budde, G. Lüpke, E. Chen, X. Zhang, N. H. Tolk, L. C. Feldman, E. Tarhan, A. K. Ramdas, and M. Stavola, Phys. Rev. Lett. **87**, 145501 (2001).

[17] G. Lüpke, X. Zhang, B. Sun, A. Fraser, N. H. Tolk, and L. C. Feldman, Phys. Rev. Lett. **88**, 135501 (2002).

[18] G. Lüpke, N. H. Tolk, and L. C. Feldman, J. App. Phys. **93**, 2317 (2003).

[19] B. Sun, G. A. Shi, S. V. S. Nageswara Rao, M. Stavola, N. H. Tolk, S. K. Dixit, L. C. Feldman, and G. Lüpke, Phys. Rev. Lett. **96**, 035501 (2006).

[20] D. West and S. K. Estreicher, Phys. Rev. Lett. **96**, 115504 (2006).

[21] S. K. Estreicher, T. M. Gibbons, and M. B. Bebek, J. Appl. Phys. **117**, 112801 (2015).

[22] T. M. Gibbons, S. K. Estreicher, K. Potter, F. Bekisli, and M. Stavola, Phys. Rev. B **87**, 115207 (2013).

[23] D. West and S. K. Estreicher, Phys. Rev. B **75**, 075206 (2007).

[24] R. Biswas, Y.-P. Li, and B. C. Pan, Appl. Phys. Lett. **72**, 3500 (1998).

[25] R. Car and M. Parrinello, Phys. Rev. Lett. **55**, 2471 (1985).

[26] P. Biswas, R. Atta-Fynn, and S. R. Elliott, Phys. Rev. B **93**, 184202 (2016).

[27] P. Hohenberg and W. Kohn, Phys. Rev. **136**, B864 (1964).

[28] W. Kohn and L. J. Sham, Phys. Rev. **140**, A1133 (1965).

[29] M. Valiev, E. Bylaska, N. Govind, K. Kowalski, T. Straatsma, H. V. Dam, D. Wang, J. Nieplocha, E. Apra, T. Windus, and W. de Jong, Comp. Phys. Comm. **181**, 1477 (2010).

[30] J. P. Perdew, K. Burke, and M. Ernzerhof, Phys. Rev. Lett. **77**, 3865 (1996).

[31] L. Kleinman and D. M. Bylander, Phys. Rev. Lett. **48**, 1425 (1982).

[32] The concept of k-space is not valid in amorphous or disordered materials due to the absence of translational symmetry. Here, by k-space, we refer to that of the supercell with its length (L) as the unit-cell length and the presence of periodic boundary conditions is implied. For a sufficiently large supercell, the Γ-point can be approximated by $\frac{2\pi}{L} \approx 0$, a condition that may not have been satisfied adequately in the present work.

[33] S. Nosé, Mol. Phys. **52**, 255 (1984).

[34] W. G. Hoover, Phys. Rev. A **31**, 1695 (1985).

[35] G. J. Martyna, M. E. Tuckerman, D. J. Tobias, and M. L. Klein, Mol. Phys. **87**, 1117 (1996).

[36] For systems with a moderate to large electronic gap, the adiabatic separation between the nuclear and electronic degrees freedoms can be maintained by a suitable choice of a fictitious electronic mass with a typical value in the range 500–1000 a.u. and a time step of about 5–10 a.u. (0.12–0.24 fs). The difference between the CPMD and exact or converged Born-Oppenheimer forces in such systems has been observed to be less than 10^{-4} a.u. (see Ref. 43 for details).

[37] For a Gaussian distribution $N(x_0, \sigma)$, with a mean x_0 and standard deviation σ, the majority (95 %) of the values of x are distributed between x_0 - 2.5σ to x_0 + 2.5σ, leading to an effective spread of the distribution $\Delta x = 5\sigma$.

[38] Since the infrared energy was deposited locally in Si-H bonds to excite *localized* high-frequency stretch modes of SiH/SiD, the spatial distribution of the energy is essentially *local* immediately after energy deposition. This enables us to compute the characteristic decay properties of the vibrational energy upon infrared excitation at a given temperature by subtracting the trivial contribution from the corresponding unperturbed run.

[39] The inverse participation ratio (IPR) of a vibrational normal mode with an eigenfunction ψ and frequency ω is given by, IPR (ω) = $(\sum_i |\psi_i|^4)/[\sum_i |\psi_i|^2]^2$. For a finite system consisting of N atoms, this value ranges from $1/N$ to 1, which corresponds to an ideal extended state (distributed over N atoms) and an ideal localized state (centered on a single atom), respectively.

[40] Here we refer to the time evolution of atomic nuclei via Newton's equation using the quantum-mechanical forces on atoms due to electrons and that of the classical interaction between atoms.

[41] C. P. Herrero, J. Non-Cryst. Sol. **271**, 18 (2000).

[42] A. Nitzan, S. Mukamel, and J. Jortner, J. Chem. Phys. **60**, 3929 (1974).

[43] D. Marx and J. Hutter, *Ab Initio Molecular Dynamics* (Cambridge University Press, Cambridge, UK, 2009).